Journal of Nuclear Materials 82 (1979) 392–402

THE EFFECT OF DAMAGE RATE ON VOID GROWTH IN METALS

N.M. GHONIEM
School of Engineering and Applied Science, University of California, Los Angeles, CA 90024, USA

and

G.L. KULCINSKI
Nuclear Engineering Department, University of Wisconsin, Madison, WI 53706, USA

Received 10 July 1978; in revised form 7 December 1978

The rate theory formulation of void growth was utilized to analyze the effects of damage rate on metal swelling. In particular, the swelling behavior of 316 SS was modeled as a function of temperature, over a range of displacement damage rates between 10^{-6} dpa/s and 10^{-3} dpa/s. Detailed analysis of the rate processes for point defect annihilation, migration, and loss to sinks indicated that small vacancy loops limit void growth at high damage rates. The reduction of void growth rates by vacancy emission from voids was found to be shifted towards higher temperature at higher displacement rates. In effect, the peak swelling temperature as well as the upper cutoff temperature for swelling are increased as the displacement rate is increased. The influence of constant or rate dependent nucleation conditions on the final swelling was investigated and it was shown that the initial microstructure before the growth stage essentially determines the peak swelling temperature. When appropriate empirical expressions for void and loop densities were used, the final peak swelling temperature shift agrees reasonably well with experimental data.

1. Introduction

Since the discovery of voids in irradiated metals a decade ago [1], there have been extensive experimental and theoretical investigations of this phenomenon. The detrimental impact of void swelling on the development of fast breeder reactors [2], and more recently on conceptually designed fusion reactors [3], motivated such studies. Heavy ion accelerators and electron microscopes have also been used to simulate, in a short period of time, the damage produced in reactor components over their anticipated lifetimes [4,5]. However, even though the total displacement levels can be achieved in a simulation facility, the final microstructure and swelling behavior was found to be different at the identical operating temperatures [6]. This discrepancy in behavior has been attributed to differences in damage rates (dpa/s), and is commonly expressed as a shift in the "effective" irradiation temperature [7].

The rate theory approach has been utilized to study point defect concentrations [8] and the growth of voids due to point defect fluxes in a homogeneous medium [7]. More recently, Bullouth, Eyre and Krishan (BEK) [9] have considered the effects of vacancy loops at a constant dpa rate but the influence of different damage rates has not been considered.

The objective of this paper is to use the fully dynamic rate theory [10] to analyze the effects of damage rate on void growth and the swelling of metals. The interrelationships between point defect production, absorption by different sinks, mutual recombination and thermal emission from various microstructural components will be considered. Some of the distinct features of this work are:

(1) Dynamic rather than quasi-steady-state defect concentrations have been used. This improves the accuracy of the calculations, especially in the presence of the rapidly-changing microstructure associated with vacancy loops.

(2) Rate processes contributing to microstructural changes are analyzed in detail.

(3) The exact role of vacancy loops in defect balance is investigated.

(4) The initial void radius for void growth is determined as a function of temperature and microstructure.

2. Theory and calculational procedures

In a dynamic formulation of the rate theory, Ghoniem and Kulcinski [11] expanded the BEK analysis for time-dependent irradiation conditions. Although the theory is presented extensively in refs. [9–11], a brief summary is given here.

Vacancy and interstitial fractional concentrations (C_v and C_i) are described by the following equations:

$$\frac{dC_v}{dt} = (1-\epsilon)P + P^e - P_{sv} - P_r \tag{1}$$

$$\frac{dC_i}{dt} = P - P_{si} - P_r, \tag{2}$$

where ϵ is the fraction of vacancies produced directly in vacancy loops, P is the point defect production rate, at/at s, P^e is the thermal vacancy production (emission) rate from all microstructural components, at/at s, P_{sv} is the vacancy sink removal rate, at/at s, P_{si} is the interstitial sink removal rate, at/at s, P_r is the point defect "bulk" recombination rate, at/at s = $\alpha C_v C_i$, α is the point defect recombination coefficient.

The BEK model describes vacancy loops by considering two rate equations; one for the concentration of vacancy loops (N_{vl}) and the other for the fraction of vacancies tied up in vacancy loops (q_{vl}). The rate of change of the volumetric concentration of vacancy loops is given as a balance between the production rate ($\epsilon P/\pi r_{vl}^2(0)b$) and the loss rate ($N_{vl}(t)/\tau$), i.e.,

$$\frac{dN_{vl}(t)}{dt} = \frac{\epsilon P}{\pi r_{vl}(0)^2 b} - \frac{N_{vl}(t)}{\tau}, \tag{3}$$

where $r_{vl}(0)$ is the initial vacancy loop radius (≈15 Å), b is the Burger's vector (cm), τ is the vacancy loop lifetime (s). This lifetime is a function of irradiation time in the sense that it depends on the state of the overall sink distribution prevailing at the instant the vacancy loop is created. From a Taylor series expansion of $\tau_{vl}(t)$, one gets

$$\tau(t) \approx -\, r_{vl}(0)/(dr_{vl}/dt)|_{[r_{vl}(0)]} \tag{4}$$

and the instantaneous radius of a vacancy loop is obtained from its rate equation given below.

$$\frac{dr_{vl}}{dt} = \frac{1}{b}\left[Z_v D_v C_v - Z_i D_i C_i - Z_v D_v C_v^e \exp\left\{\frac{[\gamma_{sf} + F_{eL}(r_{vl})]b^2}{kT}\right\}\right] \tag{5}$$

D_v and D_i are vacancy and interstitial diffusion coefficients, C_v^e is the thermal vacancy concentration, γ_{sf} is the stacking fault energy, $F_{eL}(r_{vl})$ is the elastic energy of a dislocation loop, k is the Boltzmann's constant, T is the irradiation temperature; Z_v and Z_i are the vacancy and interstitial bias factors.

The fractional production of vacancies directly into vacancy loops is ϵP while the loss rate of those vacancies is the net difference between interstitial absorption and vacancy emission on one side and vacancy absorption on the other. Therefore a rate equation can be written as

$$\frac{dq_v}{dt} = \epsilon P - \left\{Z_i D_i C_i \rho_d^v + Z_v D_v C_v^e \rho_d^v \exp\left[\frac{(\gamma_{sf} + F_{el}(\bar{r}_{vl}))b^2}{kT}\right] - Z_v D_v C_v \rho_d^{vl}\right\}, \tag{6}$$

where ρ_d^v is the vacancy loop line dislocation density (cm/cm^3).

Finally, the following rate equations describe the average interstitial loop ($\bar{r}_{il}$) and cavity ($\bar{r}_c$) radii as functions of irradiation time:

$$\frac{d\bar{r}_{il}}{dt} = \frac{1}{b}[Z_i D_i C_i - Z_v D_v C_v + D_v Z_v C_v(\bar{r}_{il})], \tag{7}$$

$$\frac{d\bar{r}_c}{dt} = \frac{1}{\bar{r}_c}[D_v C_v - D_i C_i - D_v C_v(\bar{r}_c)], \tag{8}$$

where

$$C_v(\bar{r}_{il}) = C_v^e \exp\left\{-\frac{(\gamma_{sf} + F_{el}(\bar{r}_{il}))b^2}{kT}\right\} \tag{9}$$

and

$$C_v(\bar{r}_c) = C_v^e \exp\left\{\frac{(2\gamma/\bar{r}_c - p)b^3}{kT}\right\} \tag{10}$$

are the vacancy concentrations near the surface of an average interstitial loop and void, respectively. γ is the cavity surface energy and p is the internal gas pressure.

Assuming that the number of void nuclei per cm^3 (N_c) has reached a saturation value, which can be determined from experiments and does not change with irradiation, the macroscopic swelling is given by

$$\frac{\Delta V}{V} = \tfrac{4}{3}\pi(\bar{r}_c)^3 N_c. \tag{11}$$

The resulting system of stiff non-linear first order ordinary differential eqs. (1)–(3) and (6)–(8) is solved by the GEAR program [12], and incorporated into a FORTRAN computer code, TRANSWELL [13]. This code has been developed to solve the rate equations under a variety of irradiation conditions. A newly developed plotting routine, PL3D [14], has been coupled with TRANSWELL to allow plotting of the information in three dimensional form as well as contour graphs.

Throughout the present analysis, the following assumptions were adopted.

(1) At a given temperature, there is a critical average void radius that starts to grow under irradiation. At high temperature, this critical size is larger because of the surface emission of vacancies. In the present computations, we empirically determine the size at which a void survives over a wide range of temperatures and displacement rates.

(2) The initial edge dislocation density is set at $\rho_d^0 = 10^8$ cm/cm^3. This value is not changed with dose and is appropriate for solution treated steels.

(3) No gas generation during irradiation is included.

(4) The nucleation of both loops and voids is assumed to be complete before the FDRT simulation was started. The temperature dependence of the void (N_c), and interstitial loop (N_{il}) density is given as

$$N_c = N_C^0 \sqrt{P} \exp\{(\Delta E_c + \Delta G)/kT\}, \tag{12}$$

$$N_{il} = N_{il}^0 \sqrt{P} \exp\{(\Delta E_{il} + \Delta G)/kT\}, \tag{13}$$

where N_C^0, N_{il}^0, ΔE_c and ΔE_{il} are empirical constants and ΔG is a function of the dpa rate. Eqs. (12) and (13) reduce to the BEK values (dose rate independent) for $\sqrt{P} = 1$ and $\Delta G = 0$ at 10^{-3} dpa/s. The square root dependence of the number densities on the displacement rate and the excess activation energy ΔG are introduced to study the effect of initially nucleated microstructure on metal swelling. The results investigated in sections 4.1–4.4 are for examples that are preconditioned to the same initial microstructure regardless of the displacement rate. The effects of the displacement rate on the initial number densities are discussed in section 4.4.

3. Method of analysis

The model is used to calculate:

(1) average void size and percent swelling,
(2) point defect concentrations and fluxes,
(3) rate processes:
  a. vacancy thermal emission rates,
  b. sink removal rates,
  c. point defect recombination rates,
(4) microstructural development:
  a. vacancy loop line dislocation density,
  b. interstitial loop line dislocation density,
  c. total dislocation density,
  d. effective void sink strength ($4\pi R_c N_c$).

The different components of the microstructure change as a function of irradiation time by the absorption and emission of point defects. If the microstructure is known at a given point of the irradiation, one can then calculate various emission and removal rate processes, which in turn determine point defect concentrations and fluxes to all microstructural components for the next time step. Void growth rates can then be computed and the final swelling calculated. Of course, the previous description is an overall picture and the non-linear feed-back effects are handled by the numerical solution.

In this study, the effects of displacement rate, from 10^{-6} to 10^{-3} dpa/s, on the growth of voids in 316 SS is studied in detail. The materials parameters (including void and loop nucleation parameters) outlined by BEK [9] and a cascade collapse efficiency of 4.4% are used throughout this work. Fig. 1a shows a three-dimensional plot of swelling versus irradiation temperature and dose at 10^{-3} dpa/s. On the other hand, fig. 1b gives the contour plots of the same case for constant swelling. A comparison of the FDRT with experimental data has been discussed elsewhere [10] and it was shown that there is reasonable agreement at 10^{-3} dpa/s.

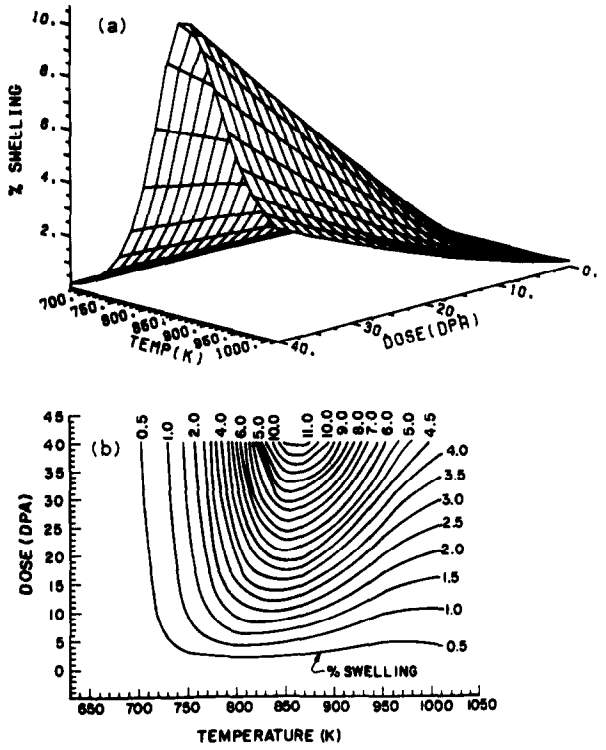

Fig. 1. Predicted swelling in 316 stainless steel bombarded with heavy ions at 10^{-3} dpa/s ($\epsilon = 0.044$). (Dose rate independent nucleation conditions.)

4. Results and discussion

A summary of the calculated swelling curves for 316 SS at various dpa rates and temperatures is given in fig. 2 at a damage level of 40 dpa. The analysis of these curves will follow shortly but it is worthwhile to first point out some of the more important qualitative features of the swelling behavior. There are three main observations.

(1) The higher the displacement rate, the lower the peak swelling.

(2) The higher the displacement rate, the higher the temperature above which no further growth occurs.

(3) The temperature of the peak swelling generally increases with dpa rate.

An explanation for these general observations can only be made by a detailed consideration of the defect concentration and flux parameters. We will now treat each of the above topics separately.

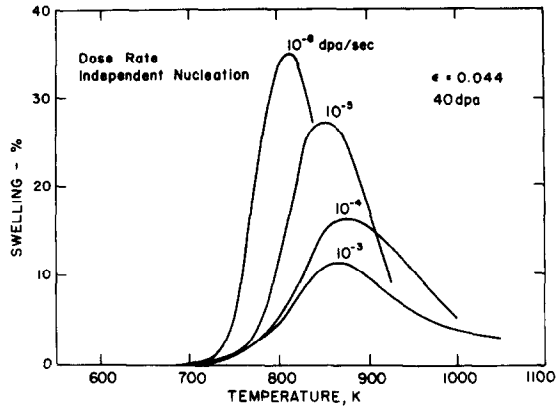

Fig. 2. Effect of displacement rate on swelling of 316 stainless steel for dose rate independent nucleation conditions.

4.1. Effect of damage rate on swelling for dose rate independent nucleation conditions

One of the most striking features of fig. 2 is the reduction in the swelling in general, and the peak swelling in particular, with increasing dpa rate. The peak swelling is shown in fig. 3 and it reveals that the values can be reduced by ≈25–35% per factor of ten increase in dpa rate.

The general reduction of swelling at temperatures below the peak value can be explained by considering eq. (8) in a slightly different format. This equation gives an approximate measure of the final swelling level, since it gives the magnitude of void growth rate.

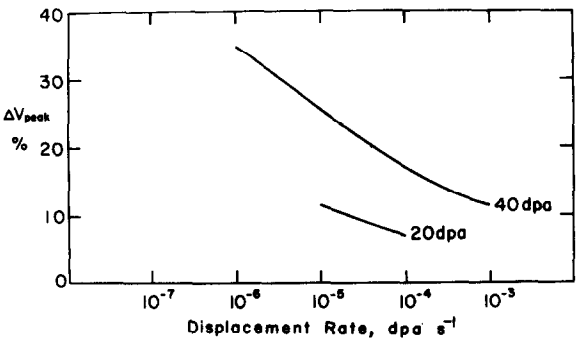

Fig. 3. Peak swelling in 316 SS as a function of dose rate. (Dose rate independent nucleation conditions.)

Table 1
Comparison of microstructural response of 316 SS irradiated at 800 K

Parameter	Units	DPA rate (s^{-1}) [a]			
		10^{-6}	10^{-5}	10^{-4}	10^{-3}
Bias flux, $(\phi_r - \phi_i)/r_c$	Å/dpa	14.181	3.781	0.997	0.690
Emission flux ϕ_e/r_c	Å/dpa	11.176	1.644	0.223	0.023
Void growth rate $\dot{r}_c$	Å/dpa	3.005	2.137	0.774	0.667
Vacancy conc., C_v		8.632×10^{-10}	3.354×10^{-9}	1.004×10^{-8}	9.548×10^{-8}
Interstitial conc., C_i		5.092×10^{-14}	2.137×10^{-13}	6.542×10^{-13}	6.303×10^{-12}
Void sink density, $4\pi r_c N_c$	cm^{-2}	1.051×10^{11}	7.43×10^{10}	5.711×10^{10}	5.584×10^{10}
Int. loop density, ρ_d^{il}	cm^{-2}	1.56×10^{11}	8.328×10^{10}	7.029×10^{10}	6.453×10^{10}
Vac. loop density, ρ_d^{vl}	cm^{-2}	1.190×10^{11}	6.371×10^{11}	2.472×10^{12}	2.586×10^{12}
Free vacancy prod. rates [b]	at/at · s				
By irradiation		95.600	95.600	95.600	95.600
By emission		13.917	4.147	1.438	0.149
Total		109.517	99.747	97.058	95.749
Free vacancy loss rates [b]	at/at · s				
To vac. loops		38.480	80.034	92.96	92.460
To voids		33.960	9.333	2.15	1.997
To inter. loops		37.380	10.462	2.64	3.307
Recombination		0.0042	0.0039	0.004	0.033
Total		109.82	99.823	97.759	96.798
Emission of vacancies [b]	at/at · s				
By edge dislocations		0.003	3.115×10^{-4}	3.115×10^{-5}	3.115×10^{-6}
By cavities		3.598	0.265	0.0212	2.079×10^{-3}
By vacancy loops		6.909	3.367	1.396	0.146
By interstitial loops		3.408	0.245	0.0207	0.190×10^{-2}
Total		13.917	4.147	1.438	0.150
Swelling (at 40 dpa)	%	32.88	11.64	5.28	4.94

[a] No swelling observed at 800 K for 10^{-7} dpa/s,
[b] Percent of interstitial production rates.

Restating eq. (6) we have,

$$\frac{d\bar{r}_c}{dt} = \frac{1}{\bar{r}_c}[\phi_v - \phi_i] - \frac{\phi_e}{\bar{r}_c},$$

where ϕ_v, ϕ_i are the vacancy (D_vC_v) and interstitial (D_iC_i) fluxes * to the void, respectively, and ϕ_e is the emission flux of vacancies from the void.

When $(\phi_v - \phi_i)$ is positive and greater than ϕ_e the void will grow. At high temperatures, where ϕ_e is large, the positive growth rate is reduced and it eventually turns negative when the void emits vacancies faster than it collects them. We will return to this point later.

To illustrate the general trends we have included in table 1 some of the important microstructural and point defect information required to understand the response of the 316 SS to several different damage rates evaluated at the same temperature (800 K) and displacement level (40 dpa). We will concentrate on the 10^{-6} and 10^{-5} dpa/s results next.

The growth rate of the average size void at 10^{-6} dpa/s, due to the bias flux term $[(\phi_v - \phi_i)/\bar{r}_c]$, is approximately 14 Å/dpa. When the dpa rate is increased by a factor of 10, to 10^{-5} dpa/s, we find that the growth due to the bias flux drops by a factor of ≈3.5 to ≈3.8 Å/dpa. The reason for this drop is

* $\phi_{v,i}$ are proportional to the actual atom fluxes, but the term 'flux' will be used here for convenience.

that while both the C_v and C_i terms increase with dpa rate, they also depend on the temperature and the value of C_i increases faster than C_v, as can be seen from table 1. Even though the bias flux drops with increasing dpa rate it is the absolute *difference* between that term and the shrinkage terms which determines $d\bar{r}_c/dt$, so we must next investigate the effect of damage rate on ϕ_e.

The rate of shrinkage of the average size void is reduced with increasing dpa rate as the net result of two opposing effects. First, because the bias flux is smaller at higher dpa rates, the net swelling is less and the average void size is smaller at a given dpa level. This smaller void size will actually result in higher emission rates since $\phi_e \alpha \bar{r}_c^{-1} \exp(\text{const}/\bar{r}_c)$. However, because the time required to accumulate 1 dpa is a factor of 10 less at 10^{-5} dpa/s and the emission rate is essentially constant with time, the net effect is a reduction in the dose integrated vacancy flux by roughly a factor of 7.

It is noted from table 1 that the void sink density ($4\pi r_c N_c$) drops slightly while the vacancy loop density increases with higher dose rates. This has the effect of increasing the ratio of the bias to emission vacancy fluxes as we go to higher dose rates. It can also be observed from the same table that the contribution to total vacancy production from thermal sources decreases with higher dose rates. This is essentially due to the diminishing role of thermally emitted vacancies at high displacement rates. Most vacancy losses occur at vacancy loops, especially for the higher displacement rates. This reduces vacancy fluxes going to voids and causing them to grow. This final point can be observed from the decreasing values of swelling as the displacement rate is increased.

Void growth results are summarized in fig. 4. It can be seen from that figure, that the shrinkage term becomes negligible above 10^{-4} dpa/s and the growth per dpa is entirely determined by the bias flux term.

One word of caution is necessary here and that is the prior analysis was made at a given dpa level and the growth rates at other dpa levels will be slightly different. However, the same qualitative features are preserved above the initial transient fluence of $\approx$1 dpa.

The next logical question is why does the increased damage rate actually lower the bias flux when the vacancy and interstitial concentrations are higher? Intuitively, one would expect the opposite behavior. To

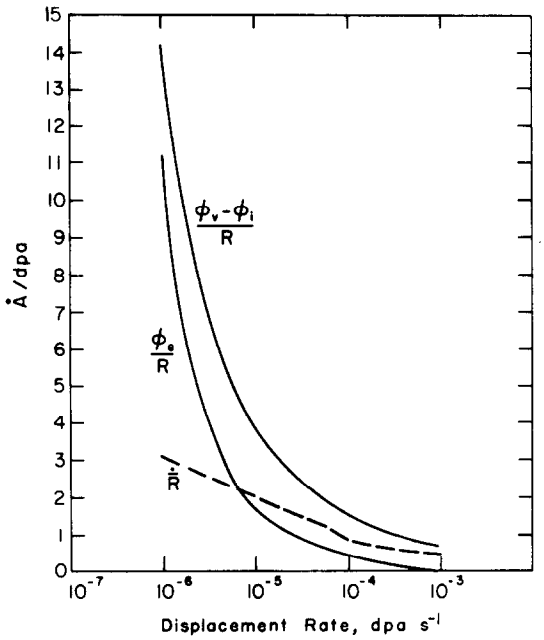

Fig. 4. Void growth and shrinkage rates in 316 SS at 800 K and 40 dpa. (Dose rate independent nucleation conditions.)

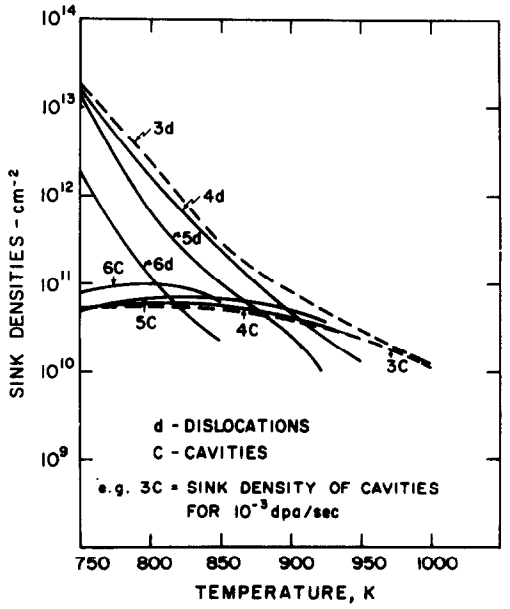

Fig. 5. Sink densities at various displacement rates as function of irradiation temperature in 316 SS. (Dose rate independent nucleation conditions.)

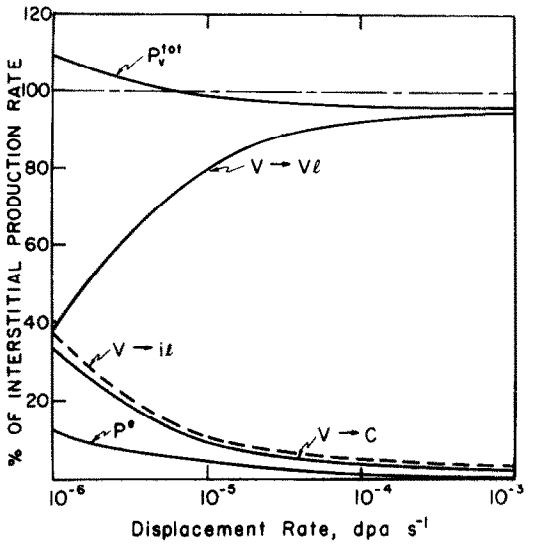

Fig. 6. Various sink loss rates of point defects in 316 SS at 800 K and 40 dpa. (Dose rate independent nucleation conditions.)

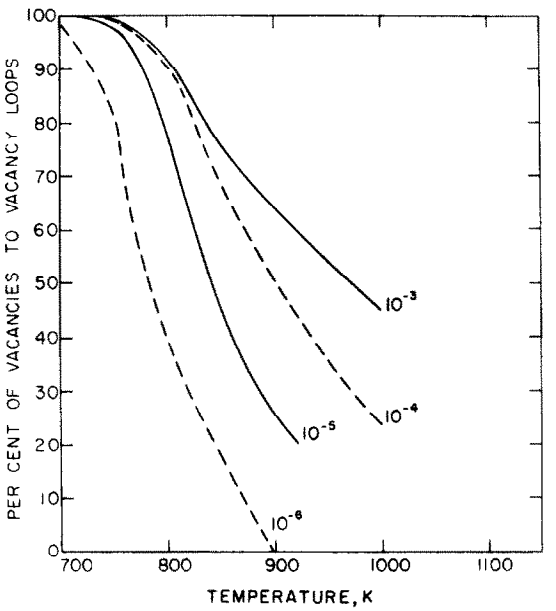

Fig. 7. Effect of displacement rate and temperature on the loss of vacancies to vacancy loops. (Dose rate independent nucleation conditions.)

understand this effect we need to examine the effect of displacement rate on the sink densities for the various defects. We have plotted in fig. 5 the dislocation and void sink densities for various dpa rates and temperatures. The first point to note is that at low temperatures the dislocation loops are the dominant sinks for defects. Secondly, the magnitude of the dislocation sink density increases with damage rate and this is mainly due to the increase in vacancy loop concentration. Previous analysis of the vacancy loop density shows that it is directly proportional to the production rate, eq. (11). The higher sink density means that even though the concentration of the vacancies in the matrix will be increased due to the higher dpa rate, a larger fraction of the defects (both vacancies and interstitials) will go to the vacancy loops, thus reducing the fraction ending up at the void.

This latter point is illustrated in figs. 6 and 7 where we have plotted the fraction of vacancies ending up at certain sinks. Free defect recombination is negligible for an 800 K irradiation at 40 dpa. The first aspect to note is that the production rates of vacancies are normalized to the free interstitial production rate. Some of the vacancies are produced directly into vacancy loops and hence the free production of vacancies from irradiation is actually less than one. However, vacancies are also produced by thermal emission from dislocation loops and voids. At low displacement rates and high sink densities these excess vacancies actually result in an effective production rate which is greater than one for free vacancies. Eventually, at high dpa rates, this thermal emission term becomes a negligible fraction of the vacancy production and the free vacancy production rate approaches $(1 - \epsilon)P$.

The data in fig. 6 and table 1 show that at 10^{-6} dpa/s the loss to voids, vacancy loops, and interstitial loops is roughly equal. Recombination rates are negligible in this case. As the dpa rate is increased, the increased vacancy loop concentration collects more and more vacancies so that by 10^{-4} dpa/s over 90% of the vacancies (and interstitials as well) end up at the vacancy loops. Hence the vacancy loops tend to retard the increase in C_v normally associated with higher dpa rates. This retardation of C_v, due to recombination, is greater than for C_i because of the direct production of vacancies into vacancy loops.

This general effect is evident over a wide range of temperatures as is shown in fig, 7. Here we see that at low temperatures the vacancy loops completely dominate the situation and this explains why there is very

little swelling in samples irradiated at low temperatures. The effect is enhanced at high displacement rates. At higher temperatures, the loops evaporate faster and hence lose their influence, expecially at the lower dpa rates. When the displacement rate is increased to 10^{-3} dpa/s, the vacancy loops play a dominant role even at 950 K. This is due to the fact that even though the lifetime of vacancy loops is extremely short, the loops are being produced at a high enough rate to offset their disappearance by evaporation.

4.2. Effect of displacement rate on upper temperature cutoff

As explained earlier, once the ϕ_e term of eq. (7) exceeds the bias flux value, the voids can no longer grow. The temperature at which this occurs is defined as the upper temperature cutoff. The reason that this upper temperature cutoff is increased with dpa rate is that even through the value of C_v is increasing slower than C_i, the *absolute* difference between C_v and C_i increases with dpa rate. (D_v and D_i are assumed to be independent of dpa rate.) This higher absolute bias flux requires a higher emission rate to produce no net growth and this in turn requires a higher temperature. This behavior is illustrated in fig. 8 for the temperature range 700–1000 K. At the lower temperature, $(\phi_v - \phi_i) > \phi_e$ for all dpa rates. It has been found from the calculations that this inequality is only true for displacement rates of greater than 2×10^{-6} dpa/s at 900 K while at 950 K it is only true for damage rates greater than 10^{-5} dpa/s. We did not determine the upper limits for higher damage rates because the nucleation conditions for such temperatures are not well known, but the fact that voids can be found in 316 SS samples at 1000 K after 10^{-3} dpa/s bombardment [4] is consistent with our analysis.

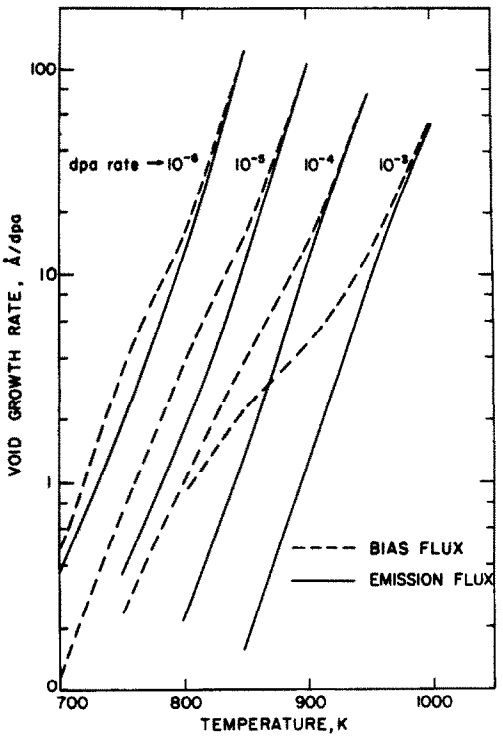

Fig. 8. Point defect fluxes at void surfaces in 316 SS as functions of temperature. (Dose rate independent nucleation conditions.)

4.3. Displacement rate effects on the peak swelling temperature

The peak swelling and its temperature dependence is one of the major experimental observations obtained from heavy ion studies. Therefore, we will consider the factors affecting this behavior. There are really two questions here:

(1) Why is the peak swelling value reduced with increasing displacement rate?

(2) Why does the peak swelling temperature increase with increasing damage rate?

Before trying to answer these questions, we will briefly discuss the factors defining the peak swelling temperature. A maximum swelling value $(\Delta V/V\%)_{max}$ does not generally correspond to the largest void growth rate. This is essentially because the void number densities decrease as the irradiation temperature is increased and one could get a larger swelling value below the peak growth temperature because of the higher void number densities.

The void growth rate as a function of both the displacement rate and irradiation temperature is shown in fig. 9. It is interesting to note that for each displacement rate, there also exists a temperature above which void growth rate becomes negative. This actually defines the high temperature swelling cutoff, and is due to the large effect of vacancy emission from the void surface.

The answer to the first question above can now be

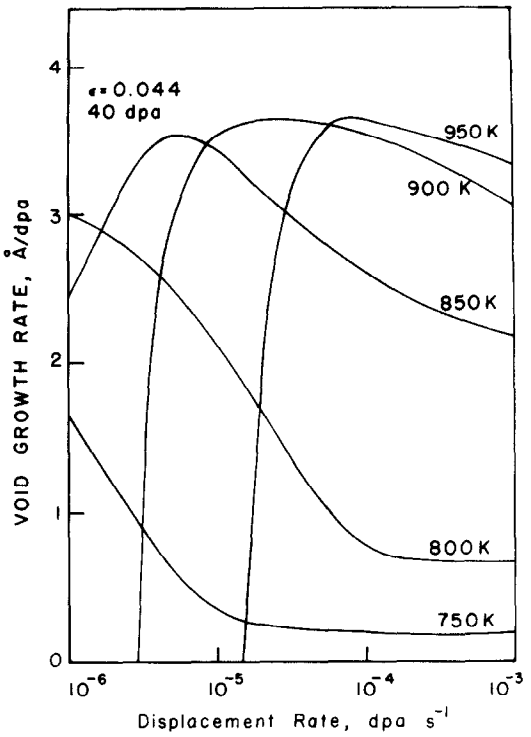

Fig. 9. Void growth rate in 316 SS as a function of displacement rate at various temperatures. (Dose rate independent nucleation conditions.)

obtained. Increasing the displacement rate increases the vacancy loop concentration, as reflected in the sink loss terms of figs. 6 and 7, and at low temperatures, this generally decreases the bias flux (fig. 4). Consequently, the net void growth rate at low temperatures is reduced with increasing displacement rate (fig. 9 for 750 K and 800 K). At temperatures above 850 K one can actually have rather high void growth rates but since the number density of voids is significantly reduced thus the total swelling is reduced.

To understand the peak swelling temperature shift to higher temperatures with increasing dose rate, we have to consider void growth rates in fig. 9. For a displacement rate of 10^{-6} dpa/s the maximum void growth rate corresponds to a temperature of 800 K. Above this temperature the void growth rate is largely reduced by thermal vacancy emission from the void surface and the number density of voids is reduced. As the temperature is further increased (at 10^{-6} dpa/s) voids start to shrink instead of grow (e.g. see curve for 900 K). When we consider higher dose rates, the effectiveness of the constant thermal emission on reducing growth rates is diminished because of the short time required to reach the desired damage level (fig. 4) and swelling will occur at higher temperatures than possible for lower dpa rates. This has the net effect of "moving" the peak swelling temperature to higher values.

4.4. *Influence of nucleation on swelling behavior*

Among the input parameters to the present rate theory model are the number densities of voids and interstitial loops. In the previous sections, it has been assumed that those initial densities will remain constant at any given temperature and that the microstructure is merely in a state of "growth". Also, the samples were all assumed to have been preconditioned to the same microstructure independent of the particular dose rate. However, as discussed in section 2, the initial microstructure can also depend on the dose rate. In this section, we investigate the influence of dose rate dependent defect densities on void swelling in stainless steel.

Experimental observations of void and dislocation loop number densities have been reported in terms of an Arrhenius function [9,15] with a pre-exponential and a thermal activation energy [eqs. (12) and (13)]. The experimentally determined activation energy for the void number density in 316 SS varies between 0.625 eV [9] to 1.1 eV [15]. A theoretical investigation by Makin [16] suggests a square root dependence on dose rate for the interstitial loop pre-exponential and we assume the same rate dependence is true for void nucleation.

The pre-exponentials and activation energies ΔE_c and ΔE_i [in eqs. (12) and (13)] have been previously determined by BEK [9] for best fit with experimental data at 10^{-3} dpa/s. We have determined appropriate values of ΔG that correspond to a reasonable agreement with temperature shift data of Bates and Straalsand (neutron irradiation at 10^{-6} dpa/s [16]) and Williams (ion irradiation at 10^{-3} dpa/s [4]) of 316 SS. The computed values of ΔG are given by the equation

$$\Delta G = 0.084 \log\left[\frac{10^{-3}}{P}\right] \text{eV}, \quad 10^{-6} \leqslant P(\text{dpa/s}) \leqslant 10^{-3}. \tag{14}$$

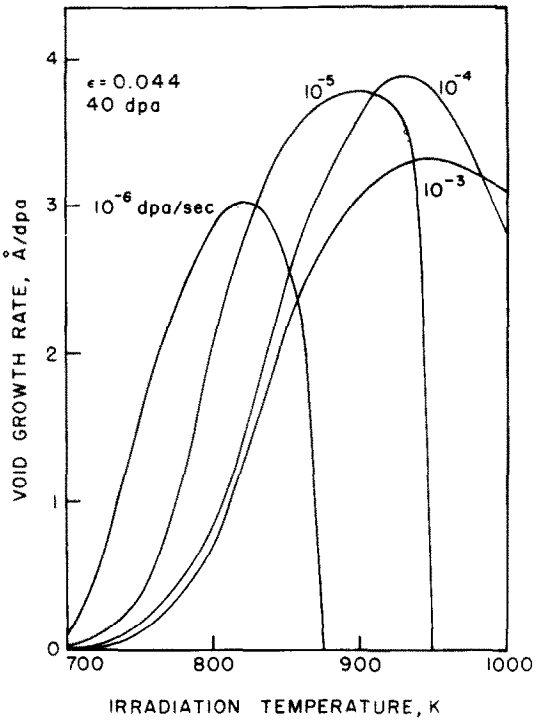

Fig. 10. Void growth rate in 316 SS as a function of temperature for various displacement rates. (Dose rate dependent nucleation conditions.)

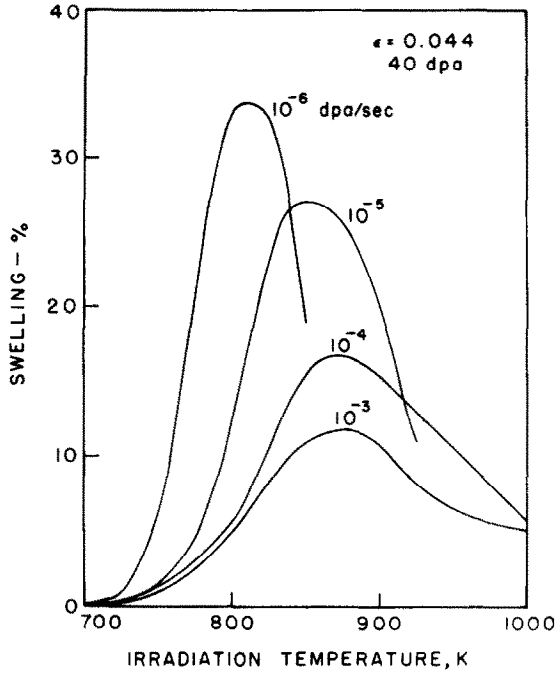

Fig. 11. Temperature dependence of swelling in 316 SS at different displacement rates for dose rate dependent nucleation conditions.

Void growth rates at 40 dpa as a function of temperature, are shown in fig. 10 for different displacement rates, with the initial void and loop densities determined from eqs. (12)–(14). The data can again be explained by considering vacancy loop and thermal emission behavior as functions of both temperatures and displacement rate. It is interesting to note, however, that between 10^{-6} dpa/s and 10^{-3} dpa/s the peak void growth rate shifts upwards by about 130°C, whereas the corresponding peak temperature for swelling shifts by only about 65°C (fig. 11). This value of the temperature shift is in accord with experimental findings on 316 SS [4,17]. It is very important to note that by comparing figs. 2 and 11 one finds the swelling results are not very sensitive to the dose rate dependence of the initial microstructure. It is therefore concluded that it is the temperature dependence of the nucleation conditions, not the dose rate effects, which are responsible for the smaller temperature shift than predicted by void growth considerations alone in ref. [7].

5. Summary and conclusions

The theory formulation of the rate theory developed by Bullough, Eyre and Krishan [9] and expanded for point defect time behavior by Ghoniem and Kulcinski [10,11] have been utilized to investigate the effect of damage rate on void growth in metals. The analysis presented here shows the simple peak swelling temperature shift formulas based on void growth alone are not adequate to explain all of the effects of a higher damage rate on the temperature dependent swelling.

It has also been shown that under certain conditions (usually low temperatures and high displacement rates) vacancy loops act as the main sink for both vacancies and interstitials, enhancing their mutual recombination. This tends to push the observed swelling to higher temperatures.

In the present investigation, it has been demonstrated that the effectiveness of thermal emission on void growth rates is also reduced with increasing dose rates. Therefore, the maximum void growth rate occurs at a higher temperature when the displacement damage rate is increased.

The upper temperature cutoff for swelling is realized when the net bias flux is less than the emission flux ($\phi_v - \phi_i \leq \phi_e$). At higher temperatures, ϕ_e is large due to the increase in the self diffusion coefficient ($D^s = D_v C_v^e$). On the other hand, it is shown that metals irradiated at higher displacement rates contain higher vacancy concentrations and consequently, a higher temperature is needed to counterbalance the absolute value of ($\phi_v - \phi_i$).

Finally, the influence of the initial void and dislocation loop densities on the swelling behavior has been found to significantly affect the peak swelling temperature. When appropriate empirical representations for the number densities are used, a reasonable agreement between the calculated and observed temperature shift data was thus obtained. The temperature shift of the maximum void growth rate between reactor and accelerator conditions is $\approx 130\,^{\circ}C$, while the actual peak swelling temperature shift is only $\approx 65\,^{\circ}C$ due to the temperature effect on the nucleation conditions.

Acknowledgement

This work was partially supported by the Division of Laser Fusion Energy, Department of Energy, and the School of Engineering and Applied Science, UCLA.

References

[1] C. Cawthorne and E.J. Fulton, Nature 216 (1966) 575.
[2] P.R. Huebotter and T.R. Bump, USAEC Report CONF-710601 (1972) p. 84.
[3] G.L. Kulcinski, University of Wisconsin Fusion Design Memo UWFDM-186 (1976).
[4] T.M. Williams, in: Proc. BNES Europ. Conf. Voids Formed by Irradiation of Reactor Materials, Eds. S.F. Pugh, M.H. Loretto and D.I. Norris (1971) p. 205.
[5] J.A. Sprague et al., J. Nucl. Mater. 54 (1974) 286.
[6] J.E. Westmoreland et al., Radiation Effects 26 (1975) 1.
[7] A.D. Brailsford and R. Bullough, J. Nucl. Mater. 44 (1972) 121.
[8] H. Wiedersich, Radiation Effects 12 (1972) 121.
[9] R. Bullough, B. Eyre and K. Krishan, Proc. Roy. Soc. A346 (1975) 81.
[10] N.M. Ghoniem, Ph.D. Thesis, University of Wisconsin, Madison, USA (1977).
[11] N.M. Ghoniem and G.L. Kulcinski, Radiation Effects 39 (1978) 47.
[12] A.C. Hindmarch, Lawrence Livermore Laboratory Report UC10-30001 (1974) rev. 3.
[13] N.M. Ghoniem and G.L. Kulcinski, University of Wisconsin Fusion Design Memo UWFDM-181 (1976).
[14] N.M. Ghoniem and E. Anderson, University of Wisconsin Fusion Design Memo UWFDM-211 (1977).
[15] B.L. Eyre, USERDA Report CONF-751006-P2 (1975) p. 729.
[16] M.J. Makin, Phil. Mag. 19 (1969) 1133.
[17] J.F. Bates and J.L. Straalsund, Hanford Engineering Development Laboratory Report HEDL-TME-71-139 (1971).